NASA Technical Memorandum 83336

Transient Difference Solutions of the Inhomogeneous Wave Equation: Simulation of the Green's Function

Kenneth J. Baumeister
Lewis Research Center
Cleveland, Ohio

Prepared for the
Eighth Aeroacoustics Conference
sponsored by the American Institute of Aeronautics and Astronautics
Atlanta, Georgia, April 11-13, 1983

NASA

TRANSIENT DIFFERENCE SOLUTIONS OF THE INHOMOGENEOUS WAVE EQUATION: SIMULATION OF THE GREEN'S FUNCTION

Kenneth J. Baumeister

National Aeronautics and Space Administration
Lewis Research Center
Cleveland, Ohio 44135

Abstract

A time-dependent finite difference formulation to the inhomogeneous wave equation is derived for plane wave propagation with harmonic noise sources. The difference equation and boundary conditions are developed along with the techniques to simulate the Dirac delta function associated with a concentrated noise source. Example calculations are presented for the Green's function and distributed noise sources. For the example considered, the desired Fourier transformed acousitic pressures are determined from the transient pressures by use of a ramping function and an integration technique, both of which eliminates the nonharmonic pressure associated with the initial transient.

Nomenclature

A^*_o	area, m^2
A	amplitude
a	range of source, eq. (41)
B	function of ω
b	ramping coefficient, eq. (33)
c	dimensionless speed of sound, c^*/L^*f^*
c^*	speed of sound, m/sec
F	dimensionless force $F^*/(\rho^*_o f^* c^*)$
F_x	dimensionless component of force in x direction
f	function
f^*	frequency, Hz
G	time dependent Green function
g	steady-state Green function
H	unit step function
I	index of last grid point
I_{cycle}	total number of time increments per cycle of base frequency
i	$\sqrt{-1}$
k	time index
L^*	characteristic length, m
L_f	Fourier transform operator
n	harmonic number
$\bar{n}$	unit outward normal at boundary
P	time-dependent dimensionless acoustic pressure $P^*/\rho^*_o c^{*2}$
p	spatially dependent steady-state acoustic pressure
Q	dimensionless mass source, $Q^*/f^*\rho^*_o$
S	dimensionless time dependent acoustic source, eq. (6)
s	spatially dependent acoustic source, eq. (9)
T^*	period, sec $(1/f^*)$
t	dimensionless time, t^*/T^*
t^*	time, sec
Δt	time increment
Δt_s	maximum stable time increment, eq. (24)
U	acoustic velocity, U^*/c^*
x	space coordinate, x^*/L^*
x_s	location of source
Δx	space increment
α	$(c\ \Delta t/\Delta x)^2$
β	parameter, eq. (A3)
δ	Dirac Delta function
ζ	exit impedance, eq. (15)
ρ^*_o	ambient density, kg/m^3
σ	$(c\ \Delta t/\Delta x)/\zeta e$
ω	dimesionless frequency $(n\omega^*/f^*)$
ω_1	2π
ω_n	$n2\pi$
ω^*_1	dimensionless angular frequency, rad/sec

Superscripts

*	dimensional quality
k	time index

Subscripts

i	space index
n	harmonic number

Introduction

Finite difference and finite element numerical solutions to the homogeneous wave equation have been successfully used to predict harmonic radiation from turbofan engine inlets[1,2] as well as internal propagation in a wide variety of complex hard and soft wall ducts, as cited in the summaries of references 3 and 4. In these solutions, the noise sources were decoupled from the propagation problem which reduced the more general inhomogeneous wave equation(ref. 5, eq. I.20) to a simpler homogeneous form. In the homogeneous form, a known or estimated pressure profile is used as a boundary condition at some location, such as the fan face in a turbofan engine, and the propagation of this pressure wave is predicted from a solution of the wave equation or the more general linearized gas dynamic equations.

Numerical solutions to the inhomogeneous equations could be useful in studying the coupled interaction of the noise source and sound field for a wide class of practical problems. For example, the noise generated by propellers[6], fan blades[7], and shear flow[8,9] can be modeled by solutions to the inhomogeneous wave equation utilizing monopoles, dipoles, and quadrupoles as the noise sources. As with the numerical approach to the homogeneous equations, numerical solutions of the inhomogeneous equations would focus on sound propagation with complex geometries and flow patterns[10,11] which would be difficult to handle with analytical methods.

Some inhomogeneous problems of current interest, such as a turboprop noise field, require three dimensional solutions to the sound field. Consequently, the transient finite difference solution to the wave equation will be employed in the present paper. Customarily, in the bulk of the past numerical studies[3,4], the pressure and acoustic velocities were assumed to be simple harmonic functions of time. In this case, the time independent wave equations can be used. The matrices associated with the numerical solutions to the time independent equation (called steady-

state solutions herein) must be solved exactly using such methods as Gauss elimination. As a result, large arrays of matrix elements must be stored, which prohibits realistic three dimensional solutions to the wave equation. In contrast, the transient analysis begins with a harmonic noise source radiating into an initially quiesent environment. Next, an explicit iteration method calculates stepwise in real time to obtain the transient as well as the steady-state solution of the acoustic field. Advantageously, this approach has been chosen because the matrix storage requirements are completely eliminated in the transient solution.

Maestrello, Bayless, and Turkel[12] have studied transient finite difference solutions to the linearized continuity and momentum equations for a pulse noise source which propagates in a jet (sheared flow). They found amplification of the noise source due to shear. Up to the present time, however, transient finite difference solutions have not been applied to the harmonic ($e^{-i\omega^* 1 t^*}$) form of the inhomogeneous wave equation. Therefore, the primary purpose of this paper is to develop the inhomogeneous tranisent finite difference equations in one dimension for a harmonic sound source with the Sommerfeld radiation boundary condition[13], and to verify the theory with appropriate examples.

The transient numerical procedures employed herein are intended to simulate the analytical Fourier transformed form of the acoustic solutions, where all the acoustic parameters vary as $e^{-i\omega^* 1 t^*}$. The steady-state numerical solutions exactly simulate the analytical results. Unfortunately, this is not the case for the transient solution. Basically, the analytical and steady-state numerical theories assume the harmonic forcing function has begun at time equal to minus infinity. On the other hand, the transient solution abruptly begins the harmonic oscillation at time equal to zero. Clearly,

$$L_f\left[e^{-i\omega_1^* t^*}\right] \neq L_f\left[H(t^*)\, e^{-i\omega_1^* t^*}\right] \tag{1}$$

where L_f is the Fourier transform operator[ref. 14, p. 28] and H represents the unit step function. Symbols are defined in the Nomenclature. The symbols with an asterisk represent dimensional quantities. The second purpose of this paper is to develop the steps necessary to adapt the transient solution to simulate the Fourier transform form of the solution.

Finally, analytical predictions for noise propagation from both steady and unsteady noise sources, such as a propeller, rely on the integration of a unit source represented by a free field Green's function g and the product of the magnitude of the source F^*[ref. 14, p. 743] such that

$$P^* = \int_{A_0^*} F^* g^* dA_0^* \tag{2}$$

Consequently, predictions of the free field Green's function as well as the effect of a distributed source are developed herein in two examples for code verification and assessment of numerical accuracy and stability.

Governing Equations and Boundary Conditions

The governing differential equation and boundary conditions are introduced in this section of the report. First, the scalar inhomogeneous wave equation is developed. Next, the Green function form of the equation is developed and will be used for code verification. Finally, an expression for the Sommerfield exit boundary condition is presented.

Inhomogeneous One Dimensional Wave Equation

In the absence of mean flow, the dimensionless form of the plane wave linearized gas equations can be written as[ref. 5, eq. 1.11]

Continuity (isentropic)

$$\frac{\partial P}{\partial t} + c\frac{\partial U}{\partial x} = Q \tag{3}$$

Momentum

$$\frac{\partial U}{\partial t} + c\frac{\partial P}{\partial x} = F_x \tag{4}$$

The parameters used to reduce the pressures and velocities to their dimensionless form are given in the Nomenclature. The usual notation for acoustic pressure and velocity are used. Here, Q represents a dimensionless mass source and F_x a dimensionless body force. Differentiating equation (3) with respect to time and equation (4) with respect to x, and combining yields the dimensionless wave equation

$$\frac{1}{c^2}\frac{\partial^2 P}{\partial t^2} - \frac{\partial^2 P}{\partial x^2} = S(x,t) \tag{5}$$

where the acoustic source is

$$S(x,t) = \frac{1}{c^2}\frac{\partial Q}{\partial t} - \frac{1}{c}\frac{\partial F_x}{\partial x} \tag{6}$$

The first term on the right hand side of equation (6) represents the monopole contribution while the second term represents the dipole contribution. The source will be assumed to be harmonic in nature ($e^{-in\omega^* 1 t^*}$) such that equation (5) can be written as

$$\frac{1}{c^2}\frac{\partial^2 P}{\partial t^2} - \frac{\partial^2 P}{\partial x^2} = s(x)\, e^{-i\omega_n t}\, H(t) \tag{7}$$

where

$$\omega_n = n2\pi \tag{8}$$

Only the first harmonic, $n = 1$, is considered herein. However, in the numerical data reduction section, a procedure will be presented to handle a multiple frequency source problem. Because of the introduction of complex notation for the noise source, all the dependent variables are complex.

Green Function Equation

For the purpose of checking the numerical theory, the simplest form of the source is desired.

Consequently, $s(x)$ is assumed to be of the form

$$s(x) = s(x_s)\delta(x - x_s) \tag{9}$$

and

$$s(x_s) = 1 \tag{10}$$

Thus, equation (7) can be written as

$$\frac{1}{c^2}\frac{\partial^2 p}{\partial t^2} - \frac{\partial^2 p}{\partial x^2} = \delta (x - x_s)\, e^{-i\omega_1 t}\, H(t) \tag{11}$$

This source is analogous to the analytical form treated by Morse and Ingard (ref. 14, p. 133) for which a closed form analytical solution is presented.

If the signal $e^{-i\omega_1 t}$ is assumed to be applied from time minus infinity, the time dependent pressure in equation (11) represents the Green function solution for a concentrated source. Thus, equation (11) can be written as

$$\frac{1}{c^2}\frac{\partial^2 G}{\partial t^2} - \frac{\partial^2 G}{\partial x^2} = \delta (x - x_s)\, e^{-i\omega_1 t} \tag{12}$$

In this steady-state case, all the acoustic parameters vary as $e^{-i\omega_1 t}$, that is

$$G(x,t) = g(x)\, e^{-i\omega_1 t} \tag{13}$$

and the differential equation (8) becomes

$$\frac{\partial^2 g}{\partial x^2} + \left(\frac{\omega_1}{c}\right)^2 g = -\delta (x - x_s) \tag{14}$$

Later, numerical solutions of equation (11) will be compared to analytical solutions of equation (14).

Sommerfeld Radiation Boundary Condition

The two required boundary conditions upstream and downstream of the noise source can be expressed in terms of a specific acoustic impedance defined as

$$\zeta_e = \frac{p}{\bar{n}\cdot U} \tag{15}$$

Substituting equation (15) into equation (4) yields the following relationship for the exit pressure gradient

$$\frac{\partial p}{\partial x} = -\frac{1}{c\zeta_e}\frac{\partial p}{\partial t} \tag{16}$$

For the plane wave propagation to be considered herein, $\zeta_e = 1$ (dimensionally equal to $\rho_0 c$) which is equivalent to propagation at an exit without acoustic reflections, commonly called the Sommerfeld radiation condition.

Initial Conditions

In the numerical calculations, for times equal to or less than zero, the acoustic field is assumed quiescent, that is, the acoustic pressure and velocities are taken to be zero. For times greater than zero, the application of the noise source (eq. (7)) will drive the pressures.

Difference Equations

Instead of a continuous solution for pressure in space and time, the finite-difference approximations will determine the pressure at isolated grid points in space as shown in Fig. 1 and at a discrete time steps Δt. Starting from the known initial conditions at $t = 0$ and the boundary conditions, the finite-difference algorithm will march-out the solution to later times.

The difference equations can be developed by an integration of the governing wave equation, equation (7), in the form

$$\int_{t-\Delta t/2}^{t+\Delta t/2}\int_{x-\Delta x/2}^{x+\Delta x/2}\left(\frac{1}{c^2}\frac{\partial^2 p}{\partial t^2} - \frac{\partial^2 p}{\partial x^2}\right)dx\,dt = \int_{t-\Delta t/2}^{t+\Delta t/2}\int_{x-\Delta x/2}^{x+\Delta x/2} s(x)\, e^{-i\omega_1 t}\, dx\,dt \tag{17}$$

The integration procedure is fully documented in reference 16 and is especially useful in developing equations at boundaries and for the special case of the unit impulse function.

Central Cell

Away from the boundaries, in the central cell of Fig. 1, the integration of the various terms in equation (17) yields

$$\frac{\Delta x}{c\Delta t}\left(p_i^{k+1} - 2p_i^k + p_i^{k-1}\right) - \frac{\Delta t}{\Delta x}\left(p_{i+1}^k - 2p_i^k + p_{i-1}^k\right) = s(x_i)e^{-i\omega_1 t^k}\,\Delta t\Delta x \tag{18}$$

where i denotes the space index, k the time index, and Δx and Δt the space and time mesh spacing, respectively. All the spacings are assumed constant. The time t^k is defined as $t^k = k\Delta t$.

Solving equation (18) for the new pressure p_i^{k+1} yields

$$p_i^{k+1} = 2p_i^k - p_i^{k-1} + \alpha\left[p_{i+1}^k - 2p_i^k + p_{i-1}^k\right] + S(x_i)e^{-i\omega_1 t^k} c^2\Delta t^2 \tag{19}$$

where $\alpha = (c\Delta t/\Delta x)^2$. As will be discussed shortly in conjunction with equation (24), the value of α must be chosen less than or equal to 1 for numerical stability. Equation (19) is an algorithm which permits marching out solutions from known values of pressure at times associated with k and $k-1$. The procedure is explicit since all the past values of p^k and p^{k-1} are known as the new values of p^{k+1} are computed. For the special case at $t = 0$, the difference equation for the start up is

$$p_i^1 = p_i^0 + \Delta t \left.\frac{\partial P}{\partial t}\right|_0 + \frac{a}{2}\left(p_{i+1}^0 - 2p_i^0 + p_{i-1}^0\right) + \frac{s(x_i)c^2\Delta t^2}{2} \qquad (20)$$

where p_i^0 and $\partial P/\partial t|_0$ are taken as zero, and $e^{-i\omega_1 t}$ is taken as 1 and $H(t)$ is assumed unity over the entire $\Delta t/2$ time step.

Exit Boundary Cell

The solution of equation (17) for the exit cells is fully documented[16] when $s(x)$ is zero (homogeneous solution). In this case, the algorithm for the exit pressure is

$$p_I^{k+1} = \left(2p_I^k - p_I^{k-1} + \sigma p_I^{k-1} - \left(2\sigma\, p_I^k - p_{I-1}^k\right) + S(x_I)c^2\Delta t^2 e^{-i\omega_1 t^k}\right) \Big/ (1+\sigma) \qquad (21)$$

where σ equals $(c\Delta t/\Delta x \epsilon e)$. A similar equation exists at the entrance, in this case, I goes to 1 and I-1 becomes 2.

Green's Function Equation

Assuming $s(x)$ of the form given by equations (9) and (10) and noting that $H(t)$ is identical to 1, the integration of the source term in equation (17) yields

$$\int_{t-\Delta t/2}^{t+\Delta t/2}\int_{x-\Delta x/2}^{x+\Delta x/2} s(x)e^{-i\omega_1 t}\,dx\,dt = e^{-i\omega_1 t^k}\Delta t\int_{x-\Delta x/2}^{x+\Delta x/2}\delta(x-x_s)dx = e^{-i\omega_1 t^k}\Delta t \qquad (22)$$

Therefore, by comparing the results of the integration in equation (22) to the right hand side of equation (18), if $s(x_i)$ is chosen such that

$$s(x_i) = 1/\Delta x \qquad (23)$$

then equation (19) will simulate the Green's function solution. Of course, $s(x)$ equals zero for all i values not associated with the position of the concentrated source.

Stability

In the explicit time marching approach used here, round-off errors can grow in an unbounded fashion and destroy the solution if the time increment Δt is too large or the iteration scheme is improperly posed. The von Newman method[ref. 15, p. 104] applied to the homogeneous form of equation (7) required that

$$\Delta t_s \le \Delta x/C \qquad (24)$$

This result was first derived by Courant, Friedrichs, and Levy in 1927 for a related method and, therefore, is known as the CFL condition. This criteria proved successful in the solution of equation (7). Note, for a two dimensional problem for which nonpropagating modes exist, the exit impedance can introduce an instability into the equation[17]. In this case the eigenvalue approach[ref. 18, p. 263] should be employed to determine the effect of the boundary conditions on stability.

Numerical Data Reduction

Recall, at the start of the numerical calculation, the acoustic pressures and velocities were assumed zero throughout the duct and a source begins a harmonic oscillation. The pressures will vary harmonically at all points in the duct. In order to conveniently interpret the numerical results, the time harmonic component of pressure should be removed so that only the spatial or Fourier transformed component of pressure remains.

Homogeneous Equation

Consider the solution for plane wave propagation in the absence of noise sources $(S(x,t) = 0)$ and when the pressure at a boundary $(x = 0)$ is given by

$$P(0,t) = e^{-i\omega_1 t} \qquad -\infty < t < \infty \qquad (25)$$

In this steady-state case, all the acoustic parameters are proportional to $e^{-i\omega_1 t}$ and equation (7) reduces to the Helmholtz equation. The solution for pressure is (see Appendix A, Problem 1)

$$P(x,t) = e^{-i\omega_1(t-x/c)} \qquad (26)$$

However, in the numerical simulation to this example, the boundary condition given in equation (25) becomes

$$P(0,t) = e^{-i\omega_1 t}\,H(t) \qquad (27)$$

In this case, the numerical solution will approximate (see Appendix A, Problem 2)

$$P(x,t) = e^{-i\omega_1(t-x/c)}\,H(t-x/c) \qquad (28)$$

Although only a specific example has been considered, in homogeneous problems with forcing boundary conditions, such as equations (25) or (27), the pressure $P(x,t)$ will always be proportional to $e^{-i\omega_1 t}$ provided sufficient time has elapsed so that the initial transient has passed $(t > x/c)$. Therefore, the numerical data can be reduced to a simple spatial form by dividing by $e^{-i\omega_1 t}$[16]; that is

$$p(x) = \frac{P(x,t)}{e^{-i\omega_1 t}} \qquad t > x/c \qquad (29)$$

Inhomogeneous Problems

For many sources, such as a pure monopole, numerical data reduction for the inhomogeneous wave equation could employ equation (29) because the results will be solely harmonic in time, similar in form to equation (25) and (28). However, this will not always be the case as will now be shown. Consequently the data reduction scheme employed must always be scrutinized.

For the example source considered in this paper, the analytical solution to the steady Green's function equation (14) is (see Appendix A, Problem 3)

$$g(x) = p(x) = \frac{P(x,t)}{e^{-i\omega_1 t}} = \frac{ic}{2\omega_1} e^{i\omega_1|x-x_s|/c} \qquad (30)$$

while the numerical simulation employing equation (11) yields (See Appendix A, Problem 4)

$$P(x,t) = \frac{ic}{2\omega_1} e^{-i\omega_1 t} e^{i\omega_1' x - x_s'/c} - \frac{ic}{2\omega_1} \quad t > x/c \quad (31)$$

Dividing by $e^{-i\omega_1 t}$ according to equation (29) yields

$$\frac{P(x,t)}{e^{-i\omega_1 t}} = \frac{ic}{2\omega_1} e^{i\omega_1' x - x_s'/c} - \frac{ic}{2\omega_1} e^{i\omega_1 t} \quad (32)$$

As mentioned in the introduction, it is desirable that the numerical solutions should approximate equation (30). Therefore procedures are developed to eliminate the dc component contribution in the numerical prediction of p. In this example, two new schemes for data reduction will now be employed to simulate equation (30).

Ramping Solution

The dc component in equation (31) could result from the sudden onset of the source at time $t = 0$, in contrast to the Fourier transform solution for which the source has been applied from a time of minus infinity. To reduce the dc component, an exponential ramp function $(1 - e^{-bt})$ has been applied to the source such that

$$S(x,t) = \delta(x-x_s)(1 - e^{-bt})e^{-i\omega_1 t} H(t) \quad (33)$$

In this case, the numerical simulation for the Green's function solution becomes (see Appendix A, Problem 5)

$$p(x) = \frac{P(x,t)}{e^{-i\omega t}} = \frac{ic}{2\omega_1} e^{i\omega_1' x - x_s'/c} - \frac{c}{2\omega_1}\left(\frac{b}{\omega_1}\right) e^{i\omega_1 t} \quad (34)$$

Equation (34) will approximate the analytical Green's function solution provided (b/ω_1) is chosen to be small compared to unity.

Integral Solution

For a large class of inhomogeneous problems, the use of equation (29) presents some additional dificulties. Consider, for example, a typical forcing function for the steady or unsteady (circumferential variations of steady flow) loading noises on a propeller source (ref. 14, p. 738). The propeller source can be conveniently modeled by stationary sources which turn on and off (square wave) with time (ref. 14, Fig. 11.19) to match the passing of the propeller. For this square wave source function in time, the analytical expression for pressure will contain all the harmonics ($n\omega^*$) of the blade passing frequency $e^{-in\omega^* t^*}$. The amplitudes of the various Fourier components are determined by an exponential Fourier series fit of the known (or assumed) forcing function (ref. 14, eq. 11.3.5).

To reduce numerical data which contain a spectrum of discrete harmonics resulting from the Fourier fit of the square wave, the following orthogonality condition is used.

$$p_n(x) = \int_t^{t+1} P(x,t)\, e^{i\omega_n t}\, dt \quad (35)$$

Besides yielding the individual higher harmonics, the orthogonal properties of equation (35) will eliminate the steady offset involved in the numerical example considered herein.

In employing equation (35), for convenience, the Δt from equation (28) is adjusted as follows to obtain an even number of Δt's in one period:

$$\Delta t = \frac{1.}{\text{FLOAT (IFIX}(1./\Delta t_s) + 1)} \quad (36)$$

where IFIX converts a floating point number to an interger, and where

$$I_{cycle} = \text{IFIX}\ (1./\Delta t_s) + 1 \quad (37)$$

Consequently, the following algorithm was used to numerically evaluate equation (35) to calculate $p(x)$ for $n = 1$.

$$p(x_i) = \frac{\Delta t}{2} \sum_{j=k+1}^{j=k+I_{cycle}} \left(p_i^j e^{i\omega_1 t^j} + p_i^{j-1} e^{i\omega_1 t^{j-1}} \right) \quad (38)$$

Sample Problems - Comparisons

Two examples are now presented to illustrate the numerical techniques. Both examples have analytical solutions; therefore, a direct comparison between the numerical and analytical techniques can be made. The first example presents a simulation of the Green's function. The second example presents a solution for a distributed noise source.

Example 1 - Green's Function

As our first example of the difference technique, consider the numerical solution of the Green's Function equation, (12). In this case, the finite difference equations (19) and (20) will be used in the solution with the source term equal to $1./\Delta x$ (eq. (23)) at x_s and zero elsewhere. The exact analytical solution is given by equation (32). Taking the position of the source x_s equal to zero, considering only positive values of x in the output, and dividing both sides of equation (32) by $e^{-i\omega_1 t}$, equation (32) can be rewritten as (recall $\omega_1 = 2\pi$)

$$\frac{P(x,t)}{\left[\frac{c}{2\omega_1} e^{-i\omega_1 t}\right]} = -\sin\left(\frac{2\pi x}{c}\right) + i\cos\left(\frac{2\pi x}{c}\right) - e^{i2\pi t} \quad t > x/c \quad (39)$$

For a nondimensional speed of sound of unity and Δx of .00521, the numerical and analytical results are shown in Fig. 2 for times of 0.75, 1.0, 1.25, and 1.5. At $t = 0.75$ in Fig. 2a, the initial transient has progressed three-quarters of the way to the termination point of x equal to unity. At t greater or equal to 1.0 in Figs. 2b, c, and d, the time dependent oscillatory nature of the transient form of the solution is shown. As seen in all the Fig. 2 plots, the analytical and numerical results are in excellent agreement.

Recall, the steady-state Fourier transform solution to the Green's function equation is de-

sired. In this steady-state solution, the source has been assumed turned on from time to minus infinity. The exact analytical solution, eq. (30) can be rewritten as

$$p(x) = \frac{P(x,t)}{\left[\frac{C}{2\omega_1} e^{-i\omega_1 t}\right]} = -\sin 2\pi x + i \cos 2\pi x \qquad (40)$$

Again, the normalized velocity of sound has been taken as unity.

As discussed in the previous section, the numerical approximation to this analytical solution can be obtained by either introducing a ramp function or using the integration technique defined by equation (35).

Figure 3 shows the numerical results for the exponential ramp with a coefficient of b equal to 0.5. In this case about seven time periods (t = 7) were required before the transient solution associated with the ramp died out and the steady-state Fourier transformed solution was obtained. For t greater than 7, the numerical solution remained unchanged. The analyses, equation (34), predicted an error of b/ω_1 of .08 which is the error seen in Fig. 3.

Finally, the results of the integration technique, equation (38), are shown in Fig. 4. As seen in Fig. 4, the analytical and numerical results are in exact agreement at the end of two-cycles (t = 2).

Example 2 - Distributed Source

For the case of a distributed sound source, the solution for p(x) can be represented by the integral (ref. 14, eq. 4.4.13) of the product of the source magnitude $A(x_s)$ and the Green's Function as given by equation (30). In the present example, the source strength A is assumed constant between -a and +a and zero outside this range. Thus for x greater than a,

$$p(x) = \frac{icA}{2\omega_1} e^{i\omega_1 x/c} \int_{-a}^{a} e^{-i\omega_1 x_s/c}\, dx_s \qquad (41)$$

while for x greater than -a and less than a,

$$p(x) = \frac{icA}{2\omega_1}\left[e^{i\omega_1 x/c}\int_{-a}^{x} e^{-i\omega_1 x_s/c}\, dx_s + e^{-i\omega_1 x/c}\int_{x}^{a} e^{i\omega_1 x_s/c}\, dx_s\right] \qquad (42)$$

In the specific example now considered, a is set at a value of 0.5, the amplitude A is taken as unity and the dimensionless speed of sound is assumed to be 0.5. In this case, performing the integrations in equations (41) and (42) yields the following expressions for the normalized pressure

$$(4\pi)^2 p(x) = -(1 - \cos 4\pi x) \qquad x \leq 0.5 \qquad (43)$$

$$p(x) = 0 \qquad x > 0.5 \qquad (44)$$

The parameters have been chosen so that the noise sources combine to give complete cancellation in the region outside the source.

The results of the integration technique, equation (38) are shown in Fig. 5. As seen in Fig. 5, the analytical and numerical results are in exact agreement at the end of four cycles (t = 4).

In employing the ramping technique for the distributed source, it was necessary to reduce b to 0.1 to keep an eight percent error, as was used in Fig. 3. The reduced b leads to a solution time an order of magnitude greater than the integration technique, which limits the usefulness of the ramping technique.

Concluding Remarks

The transient difference technique was successfully formulated for the one dimensional inhomogeneous wave equation with a harmonic source. The Green's function and a distributed noise source are accurately predicted by the numerical theory. The desired Fourier transformed acoustic pressures are determined from the transient pressures by use of a ramping function and an integration technique both of which eliminate the nonharmonic pressures associated with the start-up of the particular inhomogeneous source function considered herein. The integration technique is an order of magnitude faster than the ramping technique; consequently, future numerical solution should employ this technique.

Appendix A

Fourier Integral Solutions

To verify the accuracy and applicability of the numerical techniques, closed form analytical solutions will now be developed for a variety of check problems. The complex exponential form of the Fourier integral representation will be used to develop the analytical expression.

The Fourier transform of $P(x,t)$ is defined as (ref. 14, p. 28)

$$p(x,\omega) = \frac{1}{2\pi}\int_{-\infty}^{\infty} P(x,t)\, e^{i\omega t}\, dt \qquad (A1)$$

The Fourier transform of the wave equation (5) becomes

$$\frac{\partial^2 p}{\partial x^2} + \frac{\omega^2}{c^2} p = \frac{-1}{2\pi}\int_{-\infty}^{\infty} S(x,t)\, e^{i\omega t}\, dt \qquad (A2)$$

The Fourier transorms to be considered have only simple poles and vanish at $|\omega| \to \infty$. For the problems considered herein, the x and t variables can be incorporatied in a new variable $\beta = t - x/c$ and the inverse transform can be written as

$$P(x,\beta) = \int_{-\infty}^{\infty} B(\omega) e^{-i\omega\beta}\, d\omega \qquad (A3)$$

In this case, the inverse can be written directly as (ref. 14, p. 17, eq. I.2.15)

$$\beta < 0 \qquad P(x,\beta) = 2\pi i \sum (\text{residues above real } \omega \text{ axis}) \qquad (A4)$$

$s > 0 \quad P(x,s) = -2\pi i \sum$ (residues on and below real ω axis) (A5)

Problem 1 - Harmonic Pressure All Times, $-\infty < t < \infty$

For $s(x) = 0$, the solution of equation (A2) in a semi-infinite domain (no reflections) yields

$$p(x,\omega) = C_+ e^{i\omega x/c} \tag{A6}$$

The constant C_+ (forward waves) is determined by the transformation of the boundary condition, equation (25)(ref. 19, p. 321).

$$p(0,\omega) = \delta(\omega - \omega_1) = C_+ \tag{A7}$$

The inverse $P(x,t)$ of equation (A6) with C_+ as given by equation (A7) can be determined directly from the definition of the Dirac delta function(ref. 14, p. 31, eq. 1.3.24) to yield equation (26) in the body of this report.

Problem 2 - Harmonic Pressure $t > 0$

Again for $s(x) = 0$, the solution of equation (A2) in a semi-infinite domain is given by equation (A6). In this case however, the constant C_+ is determined by the transformation of the boundary condition equation (27) to give

$$p(0,\omega) = \frac{1}{2\pi}\left(\frac{1}{\omega - \omega_1}\right) = C_+ \tag{A8}$$

Considering equations (A6) and (A8), the only residue is ω_1, which lies on the real axis. Therefore, the inverse can be found directly from equations (A4) and (A5) to yield $P(x,t)$ as given by equation (28) in the body of this report.

Problem 3 - Green's Function $-\infty < t < \infty$

For a source in the form as given in equation (12), the right hand side of equation (A2) takes on the form(ref. 19, p. 321)

$$\frac{\partial^2 p}{\partial x^2} + \frac{\omega^2}{C^2} p = -\delta(x - x_s)\,\delta(\omega - \omega_1) \tag{A9}$$

The homogeneous solution for nonreflected waves in this particular example can be written as(ref. 14, p. 133)

$$p(x,\omega) = Ae^{i\omega(x-x_s)/c} \quad x > x_s$$
$$= Ae^{-i\omega(x-x_s)/c} \quad x < x_s \tag{A10}$$

for a pressure continuous across x equals x_s. There is, of course, a discontinuity in the slope of $p(x,\omega)$ at $x = x_s$. The constant A and therefore the magnitude of the discontinuity takes on the value $x = x_s$ to satisfy the right hand side of equation (A9) at $x = x_s$. Following the procedure outlined in great depth by Morse and Ingard(ref. 14, p. 133) the constant A is found to be $A = (ic/\omega)\,\delta(\omega - \omega_1)$. Again, the inverse can be easily determined from the direct use of the Dirac Delta function(ref. 14, p. 31, eq. 1.3.24) to yield $P(x,t)$ as given by equation (30) in the body of this report.

Problem 4 - Modified Green's Function $t > 0$

For a source in the form as given in equation (11), the right hand side of equation (A2) takes on the form(ref. 14, p. 30, eq. 1.3.22)

$$\frac{\partial^2 p}{\partial x^2} + \frac{\omega^2}{C^2} p = \frac{-\delta(x - x_s)i}{2\pi(\omega - \omega_1)} \tag{A11}$$

Using the approach outlined in Problem 3 the Fourier transformed pressure becomes:

$$p(x,\omega) = \frac{-C}{2(2\pi)}\left[\frac{1}{\omega(\omega - \omega_1)}\right] e^{i\omega|x-x_s|/c} \tag{A12}$$

In taking the inverse of equation (A12), two residues are at 0 and ω_1 and both lie on the real axis. Therefore, the inverse can again be found directly from equations (A4) and (A5) to yield $P(x,t)$ as given by equation (31) in the body of this report.

Problem 5 - Ramping Function $t > 0$

For a source in the form as given in equation (33) the right hand side of equation (A2) takes on the form

$$\frac{\partial^2 p}{\partial x^2} + \frac{\omega^2}{C^2} p = \delta(x - x_s)\left[\frac{1}{2\pi}\frac{i}{(\omega - \omega_1)} - \frac{i}{2\pi(\omega - \omega_1 + ib)}\right] \tag{A13}$$

The solution for the Fourier transformed pressure becomes

$$p(x,\omega) = \frac{-c}{2(2\pi)}\left[\frac{1}{\omega(\omega - \omega_1)}\right] e^{-i\omega|x-x_s|/c} + \frac{c}{2(2\pi)}\left[\frac{1}{\omega(\omega - \omega_1 + ib)}\right] e^{-i\omega|x-x_s|/c} \tag{A14}$$

In taking the inverse of equation (A14), three residues are at 0, ω_1, and $\omega_1 - ib$ and all lie on or below the real axis. Therefore, the inverse can again be found directly from equations (A4) and (A5) to yield

$$\frac{p(x,t)}{H\left(t - \frac{|x - x_s|}{c}\right)} - \frac{ic}{2\omega_1} e^{-i\omega_1\left(t - \frac{|x - x_s|}{c}\right)}$$

$$= \frac{-ic}{2\omega_1} + \frac{ic}{2}\frac{\omega_1}{\left(\omega_1^2 + b^2\right)} - \frac{c}{2}\frac{b}{\left(\omega_1^2 + b^2\right)}$$

$$- i\frac{c}{2} e^{-i\left(t - \frac{|x - x_s|}{c}\right)\omega_1} e^{-b\left(t - \frac{|x - x_s|}{c}\right)}$$

$$\times \left[\frac{\omega_1}{\omega_1^2 + b^2}\right] + \frac{c}{2} e^{-i\left(t - \frac{|x - x_s|}{c}\right)\omega_1}$$

Continued on the next page.

$$\times e^{-b\left(t - \frac{|x - x_s|}{c}\right)} \left[\frac{b}{\omega_1^2 + b^2}\right] \qquad \text{(A15)}$$

For long times, the last two terms in equation (A15) can be neglected. In addition, if b/ω_1, is assumed to be small, equation (A15) can be approximated by equation (34) in the body of this report.

References

1. Baumeister, K. J., and Horowitz, S. J., "Finite Element-Ingegral Simulation of Static and Flight Fan Noise Radiation From the JT15D Turbofan Engine," NASA TM-82936, Aug. 1982.
2. Astley, R. J., "Finite and Infinite Elements for Acoustical Radiation," Abstract 19th Annual Meeting of the Society of Engineering Science, Inc., Univ. of Missouri-Rolla, Rolla, Missouri, Oct. 1982, p. 8.
3. Baumeister, K. J., "Numerical Techniques in Linear Duct Acoustics - A Status Report," Journal of Engineering for Industry, Vol. 103, No. 3, Aug. 1981, pp. 270-281.
4. Baumeister, K. J., "Numerical Techniques in Linear Duct Acoustics - 1980-81 Update," NASA TM-82730, Nov. 1981.
5. Goldstein, M. E., Aeroacoustics, McGraw-Hill, New York, 1976.
6. Gutin, L., "On the Sound Field of a Rotating Propeller," NASA TM-1195, 1948.
7. Sharland, I. J., "Sources of Noise in Axial Flow Fans," Journal of Sound and Vibration, Vol. 1, No. 3, July 1964, p. 302.
8. Lighthill, M. J., "On Sound Generated Aerodynamically, I. General Theory," Proceedings of the Royal Society, (London), Vol. 211A, No. 1107, 1952, pp. 564-587.
9. Lighthill, M. J., "On Sound Generated Aerodynamically, II. Turbulence as a Source of Sound," Proceedings of the Royal Society, (London), Vol. 222A, No. 1148, 1954, pp. 1-32.
10. Baumeister, K. J., "Utilization Numerical Techniques in Turbofan Inlet Acoustic Suppressor Design," NASA TM-82994, Oct. 1982.
11. Baumeister, K. J., Everman, W., Astley, R. J., and White, J. W., "Application of 'Steady' State Finite Element and Transient Finite Difference Theory to Sound Propagation in a Variable Duct: A Comparison with Experiment," AIAA Paper 81-2016, Oct. 1981.
12. Maestrello, L., Bayliss, A., and Turkel, E., "On the Interaction of a Sound Pulse with the Shear Layer of an Axisymmetric Jet," Journal of Sound and Vibration, Vol. 74, No. 2, 1981, pp. 281-301.
13. Pierce, A. D., Acoustics: An Introduction to Its Physical Principles and Applications, McGraw-Hill, New York, 1981.
14. Morse, P. M., and Ingard, K. U., Theoretical Acoustics, McGraw-Hill, New York, 1968.
15. Clark, M., and Hansen, K. F., Numerical Methods of Reactor Analysis, Academic Press, New York, 1964.
16. Baumeister, K. J., "Time-Dependent Difference Theory for Noise Propagation in a Two-Dimensional Duct," AIAA Journal, Vol. 18, No. 12, Dec. 1980, pp. 1470-1476.
17. Baumeister, K. J., "Influence of Exit Impedance on Finite Difference Solution of Transient Acoustic Mode Propagation in Ducts," Journal of Engineering for Industry, Vol. 104, No. 1, Feb. 1982, pp. 113-120.
18. Richtmyer, R. D. and Morton, K. W., Difference Methods for Initial-Value Problems, 2nd ed., John Wiley and Sons, New York, 1967.
19. Carrier, G. F., Krook, M., and Pearson, C. E., Functions of a Complex Variable, McGraw-Hill, New York, 1966.

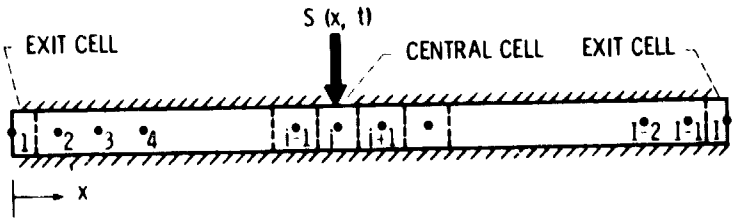

Figure 1. - Finite difference grid.

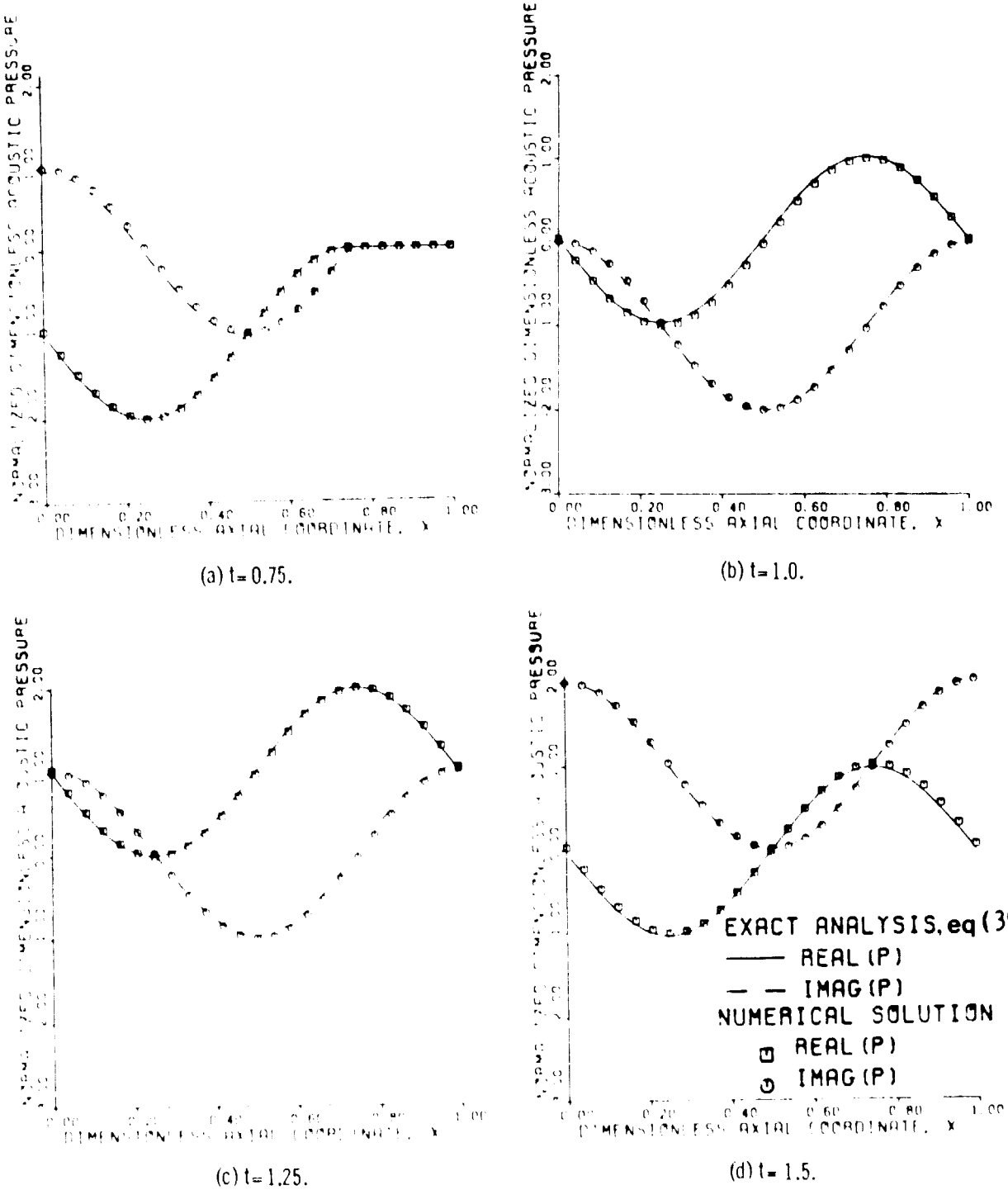

(a) t = 0.75.

(b) t = 1.0.

(c) t = 1.25.

(d) t = 1.5.

Figure 2. - Nature of Green's function and numerical solutions when source is turned on at time equal to zero.

Figure 4. - Green function solution to the inhomogeneous wave equation using the integration technieque (t=2).

Figure 3 - Green function solution to the inhomogeneous wave equation using a ramped source (b=0.5 and t=7.0).

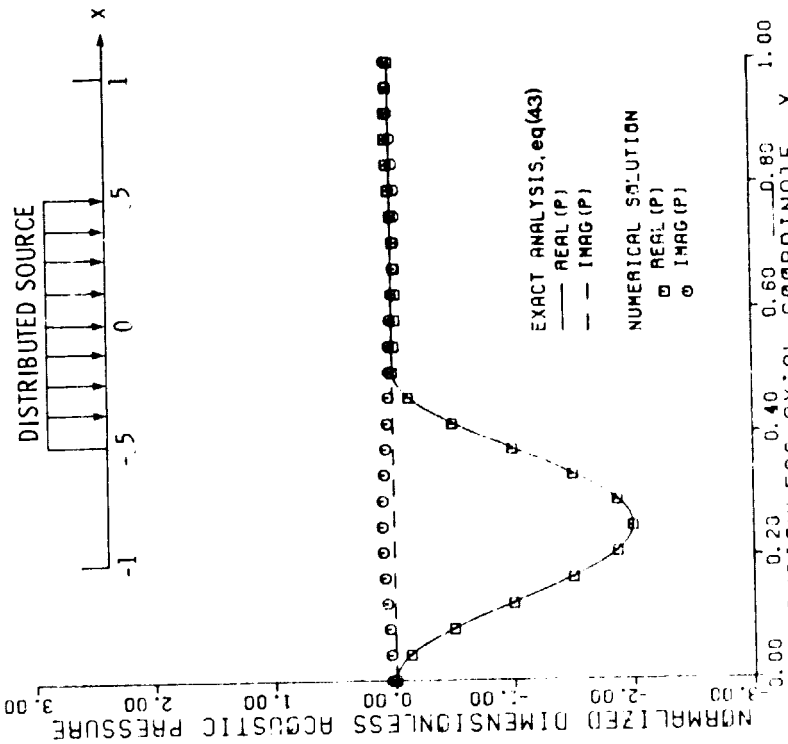

Figure 5. - Distributed source solution to the inhomogeneous wave equation using the integration technique (t=4.).